Experimental Investigation on the Removal of Recast Layer after EDM Machining

Sanjeev Kumar Vishwakarma[1] Sudhanshu Kumar[2]
[1,2]Department of Mechanical Engineering
[1,2]Maulana Azad National Institute of Technology, Bhopal, Madhya Pradesh, India

Abstract — The viability of eliminating the recast layer (RCL) utilizing etching and mechanical grinding for Ni based super alloy materials employing electrical discharge machining (EDM) is investigated in this work. EDM is a widely utilised sophisticated thermoelectric non-conventional machining technology in a variety of fields such as dentistry, medicine, and the materials which is difficult to machine by standard methods. The material is removed by melting and vaporisation, and the energy source for the material removal is heat generated by sparking. Due to improper dielectric fluid flushing, a hard and brittle coating forms on the periphery of the workpiece. If flushing is not done properly, then the molten metal re-solidifies, hardens, and adheres to the machining surface due to the cooling impact of the dielectric fluid. The layer created above the surface is called as RCL. This experiment is divided into three stages. In first stage RCL generation on the workpiece using EDM. In second stage optimizes the RCL removal, using L9 orthogonal array with Taguchi approach and create experimental plan, with different etching parameters. To find the most significant etching parameters, an analysis of variance (ANOVA) was performed. In the third stage, mechanical grinding was used to remove the RCL completely. Finally, the experiment investigates the workpiece metal removal rate and surface roughness value. The most significant parameter for all response characteristics is found to be temperature and acid composition. Metal removal rate and surface roughness value is highly affected with temperature and acid composition respectively.

Keywords: EDM, Recast layer, Taguchi method, ANOVA, MRR and Surface Roughness

I. INTRODUCTION

Electro Discharge machining is one of the most successful, practical, and lucrative unconventional machining processes for machining newly created high strength metals with high dimensional precision and low manufacturing costs. One of the primary advantages of the Electro Discharge machining technique is the ability to machine electrically conductive materials regardless of their hardness using heat energy. Material removal in the electro discharge machining method is accomplished by controlled erosion using a sequence of electric sparks. The electro discharge machining method can only be used to machine conductive materials. Electric current is discharged between two points of conductive material that are linked with appropriate polarity (positive and negative). The material to be machined is installed on the table, known as the workpiece, and the material utilised to generate the cavity, known as the tool electrode, is attached to the EDM machine's head. Between the tool electrode and the workpiece surfaces, a proper space, known as the spark gap, is maintained. A servo control device is utilised to maintain the proper spark gap between the electrodes. The average voltage detects the distance between the tool electrode and the workpiece, and this voltage is compared to the preset.

The servo motor is controlled by this difference. The tool electrode and the workpiece are submerged in dielectric fluid for maximum efficiency. The dielectric fluid is cycled through a pump and reused. Flushing is the process of injecting filtered dielectric fluid into the machining area through a nozzle. Flushing is necessary because eroded particles must be removed from the gap in order for cutting to be effective. Flushing also cools the electrode and workpiece by bringing new dielectric oil into the gap. The powerful electric field is created at the place where the surface irregularity offers the smallest gap as soon as the pulsed DC of 80-100V is transmitted through the electrodes. An electric field is created based on the applied potential difference and the space between the tool and the work piece. Electrons would be emitted from the tool if the work function or bonding energy of the electrons was lower.

From the cathode to the anode, negatively charged particles (electrons) begin to move. The electrons interact with the neutral molecules of the dielectric as both electrode surfaces are submerged in it. Electrons detach from the dielectric when they collide with neutral molecules often and quickly, making the dielectric more charged. The ionisation quickly intensifies to the point where a very narrow channel of continuous conductivity emerges.

Because of the extreme concentration, the stuff in that channel would be referred to as "plasma." Such a plasma channel would have an extremely low electrical resistance. As a result, a huge number of electrons and ions will travel from the tool to the work piece at the same time. This is referred to as electron avalanche motion. A spark is a visual representation of such electron and ion mobility. A spark is created between two electrodes, and its position is dictated by the smallest space between them, High-speed electrons collide with the workpiece and create ions on the tool. After colliding with the work and tool surfaces, the kinetic energy of electrons and ions was transformed into heat energy. As a result, the work piece is heated by the bombardment of electrons, while the tool is heated by the bombardment of ions. The spark energy raises the localized temperature of the tool and work piece to such a high level that a little quantity of material melts and vaporizes off both electrodes' surfaces at the point of spark contact. The pressure in the plasma channel increases to a very high value (about 200 atm.) due to dielectric evaporation, which prevents superheated metal from evaporating. Each spark creates an EDM chip, which is a very small hollow sphere of material made up of the electrode and the work piece material. When the pulse's off-time begins, the pressure lowers instantly, enabling the superheated metal to evaporate. The material is removed in the shape of craters that cover the whole work piece's surface.

Finally, the hollow created in the work piece resembles the tool in appearance. The process parameters should be carefully set to minimize tool wear.

The EDM microscopic examination of the machined workpiece reveals three types of layers that is Recast Layer, Heat affected zone and Converted Layer. If the molten metal from the workpiece is not flushed away appropriately by the dielectric fluid during EDM machining, a hard and brittle layer will develop. Because of the cooling impact of the dielectric fluid, the molten metal re-solidifies, hardens, and adheres to the machined surface if the flushing is not done properly. The recast layer is a layer that forms above the surface and is roughly 2.5 to 50 microns thick. The recast layers are exceedingly hard and brittle, and the surface is porous and susceptible to tiny fractures, which is not a desirable feature of a machined surface. Before employing these goods, such a surface should be removed. In order to get a superior surface quality, it is also necessary to flush. The current pulse length and energy per spark increase the thickness of the recast layer.

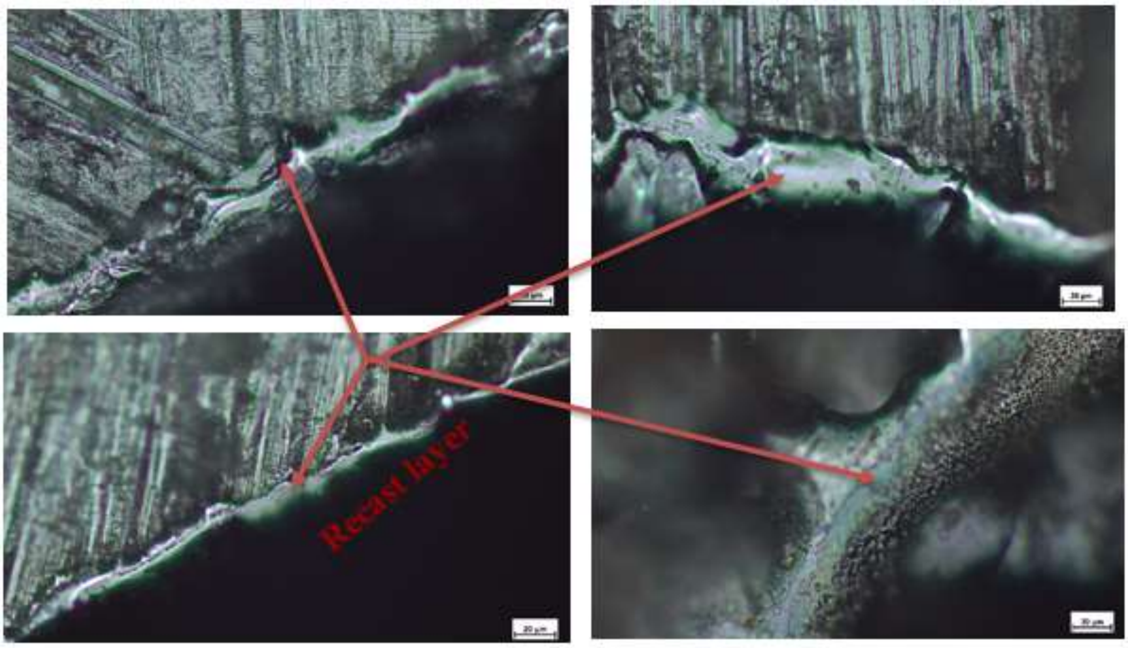

Fig. 1: Recast Layers formations images after EDM Machining

When compared to the foundation material, this layer has differing chemical and metallurgical characteristics [1, 2]. The recast layer thickness might be modest or big depending on the energy of discharges [3]. Micro fractures can also be seen in the recast layer, which can be seen in cross-sections of the tool/workpiece. Because the recast layer lowers the quality of the original surface, it is removed using a variety of processes including as lapping, grinding, and polishing. Because the size and form of the micro feature varies as a result of various finishing procedures, measuring the recast layer is a must before using any other approach to remove it [4].

Previous studies gives that following conclusion or techniques to improve the EDM process and surface profile. A proposed study that High-depth cuts are achievable with maraging steel [5, 6]. When current rises, the MRR rises with it. The strength of the spark increases as the current increases, resulting in a high metal removal rate. The roughness of the surface increases when the current is increased. Hardness will decrease as current rises. Due to the high temperature generated at high currents, crack length and crack breadth grow when current is raised. When the duty component rises, the MRR rises with it. The higher the duty factor, the more intense the spark, resulting in a high metal removal rate. Surface roughness increases as the duty factor is raised. As the duty factor increases, the spark intensity increases, causing the machining time to increase, resulting in an increase in MRR. Finally, the roughness of the surface rises. Hardness decreases as the duty factor rises. Due to the high temperature generation, when the duty factor is raised, the crack length and crack widths also rise. The MRR decreases as the pulse-on-time increases. Due to the widening of the plasma channel as the pulse-on-time increases, the strength of the spark drops, resulting in reduced metal removal. Surface roughness decreases when the pulse-on-time is increased. Hardness will rise as the pulse-on-time increases. Because of the low temperature generation at high pulse-on-time due to the expansion of the plasma channel, the crack length and crack widths rise when the pulse-on-time is raised. The average crack length decreases as the pulse-on-time increases. The thickness of the recast layer improved as the current increased [5]. The thickness of the recast layer grows as the duty factor rises. The thickness of the recast layer reduces as the pulse-on-time rises. A study carried out to investigate the machine parameters on recast layer and surface roughness [3]. Surface roughness is proportional to discharge energy, hence discharge power and duration induce a consistent rise in surface roughness. A heat impacted zone exists at all discharge energy levels. The thickness of the recast layer grows as the discharge energy increases. The produced recast layer is influenced by heat source characteristics, but the discharge duration has a greater impact.

An experimental study is conducted for the removal of recast layer with the help of etching process as well as grinding process [7]. The Taguchi experimental design was used in this study to investigate the feasibility of an EDM recast layer removal procedure, and the following research result was reached. The experiment used L18 orthogonal arrays, and the findings showed that a high voltage method could produce a wider recast layer than a negative polarity process. A thicker recast layer is also the result of a longer pulse duration. The trials also employed L9 orthogonal arrays, and the findings showed that using a corrosive including phosphoric acid and hydrochloric acid at the right temperature may considerably improve the recast layer removal rate for Inconel 718 alloy.

II. EXPERIMENTAL MATERIAL, EQUIPMENT, AND METHOD

The experiments are performed on an EDM machine as shown in figure 2 which represents complete experimental setup, where it represents electrical discharge machining and spark between the tool and the work piece. With the help of EDM machining created a cylindrical blind cavity hole onto the workpiece with constant depth and various diameters. The depth of the generated cavity is 5.5 mm and their various diameters are 8mm, 10mm and 12mm. After the completion of the EDM process thin layers are formed onto the periphery of the generated cavity, and that thin layers are called recast layers.

Fig. 2: Experimental set-up

A. *Tool and Work piece Materials*

Steel called 304 and pure electrolytic copper (99% Cu) are used to make the parts of the experiments.

Cr	Ni	C	Mn	P	S	Si	N	F_e
18-20	8-12	0.08	2.00	0.045	0.030	0.75	0.10	67-71

Table 1: Chemical composition of 304 Stainless Steel (Wt. %)

Stainless Steel 304 is made of Cr (chromium) and Ni (Nickel) and is a super alloy that is very resistant to corrosion and oxidation. There is a table no.1 that shows the chemical composition of SS 304.

Fig 3: Work piece (304 Stainless Steel) and Tool (Cylindrical Copper Electrode)

B. *Sample Preparation*

Sample preparation can be done with the help of the EDM machining process. For that we chose 304 stainless steel based on previous studies. Through the EDM process create a cylindrical blind cavities i.e. recast layer on to the workpiece. To remove that recast layer, analyse the effect of the etching process on the generated cavity. To perform the etching process only in the cavity generated area and cover all the other portion of the workpiece. For covering the un-etched portion of the workpiece, m-seal CPVC solvent cement is used as shown in figure 4.

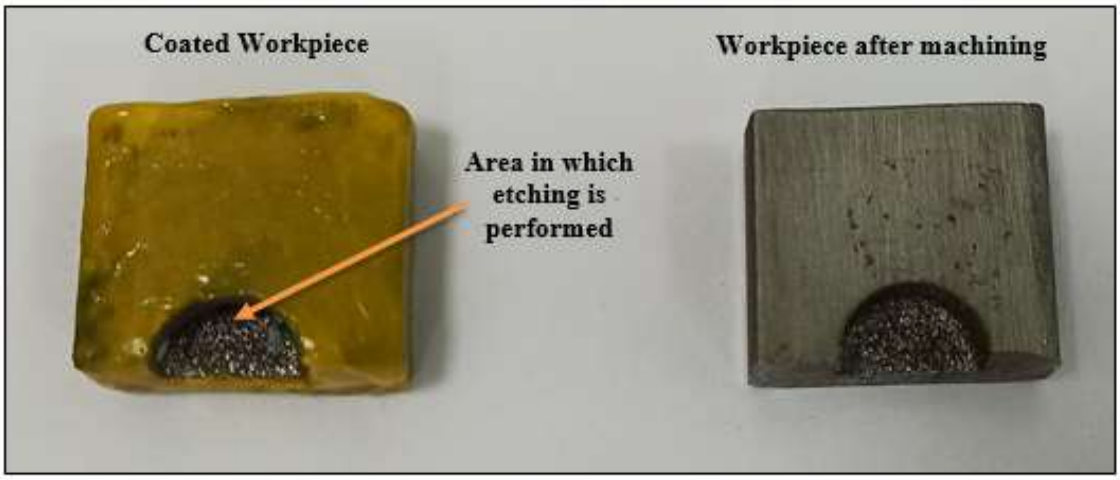

Fig. 4: Sample Preparations

C. Equipment used for experimentations

1) Vision Measuring System

The diameter of the probe or generated cavity is measured with the help of video measurement system. In this study, this surface texture of the cavity is also looked at before and after the etching process as well as after the grinding process. With the help of this machine, we go to higher magnifications and look at how well the work piece cavity is made and observed surface properties.

An interface called MSU3D-PRO can be used to see the entities through either eyepieces or a PC. Use the micro metres on the work base to move it in X and Y directions. It is also possible to take 3D measurements with a probe. The Sipcon SDM TRZ –3D has an optical magnification value upto .7X to 4.5X. The vision measuring system shown in figure 5.

Fig. 5: Vision Measuring System

2) Magnetic Stirrer with Hot Plate

In this experiment, the I Stir HP 320 magnetic stirrer model number shown in figure 6. In this there is a magnetic stirrer that has hot plates that is safe and reliable. It is also simple to use and meets all kinds of safety rules. This device is also very important if you need to mix samples for a long time, for example, for a multi-hour or overnight mix. Magnetic stirrers have a big advantage over ones that use motors. They are less noisy and more efficient. They don't have any moving parts that could break or wear out.

Fig. 6: Magnetic Stirrer with Hot Plate

3) Beakers, Pippete and Acids Solutions

There are things called beakers that hold liquid so that it can be stirred and mixed or heated. These things are called beakers. They come in a variety of shapes, sizes, and materials depending on what they're used for. They can be used again and again, or they can be thrown away. To use a pipette to get rid of, move, or measure a liquid, like water. A graduated glass tube with a large bulb that can be used to transfer liquids in precise amounts. The acids which can be used during the experimentation are hydrochloric acid (HCL), phosphoric acid (H_3PO_4) along with fixed amount distilled water (H_2O).

Fig. 7: Beakers, Pippete and Acids Solutions

4) Portable Surface Roughness Tester

The Surface roughness waveforms may be viewed on the built-in colour LCD display of the Surftest SJ-210 surface roughness measurement equipment. In addition to the calculation results, the display shows operators sectional calculation results, evaluated profiles, load curves, and amplitude distribution curves. This device can measure in any direction, including vertical and upside-down. JIS (JIS-B0601-2001, JIS-B0601-1994, JIS B0601-1982), VDA, ISO-1997, and ANSI are among the standards that the Surftest SJ-210 conforms with.

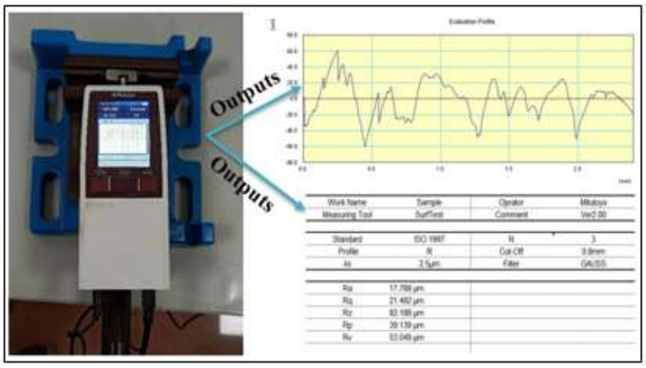

Fig. 8: Portable Surface Roughness Tester

5) Grinding Operations and Grinding Tools

For the complete removal of recast layer, a grinding operation will be performed on the workpiece for the complete removal of the recast layer. Grinding operations will be performed for a very short period of time, i.e., only for 30 seconds. Grinding tools with various diameters (8mm, 10mm, and 12mm) can be used with respective generated cavity workpiece for doing grinding operations. All the grinding tool that can use in the experiment is shown in figure 9.

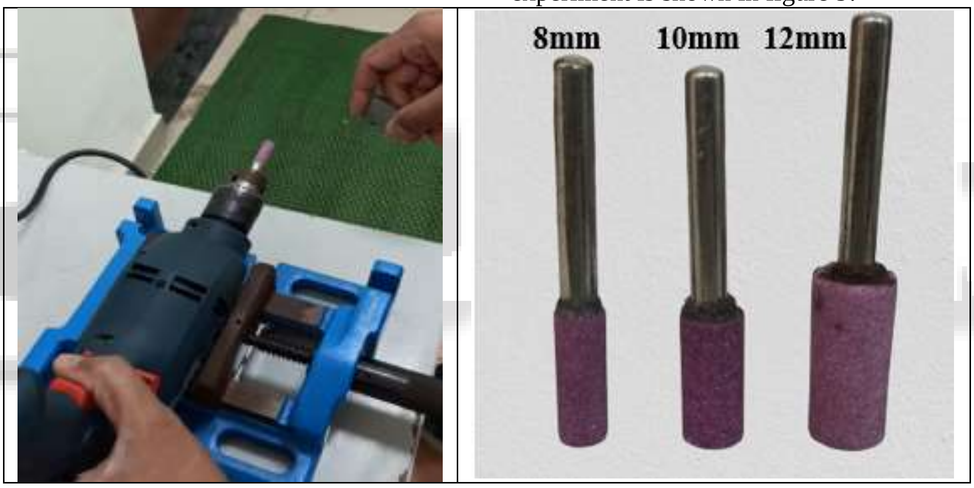

Fig 9. Grinding Operations and Grinding Tools

D. Design of experiments using the Taguchi approach

In the Taguchi technique, the orthogonal array serves as the foundation for the experimental analysis (Roy, 2001). The experiment parameter factors and their associated levels are chosen first. The ANOVA approach is then used to change the experimental findings in order to assess the influence of each parameter on the objective function.

This method also lets you look at a wide range of parameters without having to do a lot of testing, which saves both time and money. It makes it easier to find the important parameters that have the most impact on the performance characteristic value, so that minor effects can be ignored (Fraley et al., 2012).The following are the steps in the experiment.

1) The parameter variables are chosen according to the needed quality target.
2) The levels of the parameter factors are calculated.
3) The overall degree of freedom is computed and the appropriate orthogonal array is selected based on the parameter factors and levels.
4) The actual experiment may then be carried out based on the variable factor arrangement of the orthogonal array.
5) The ANOVA for signal-to-noise ratio (S/N ratio) and contribution are computed when the experimental findings are received.
6) Following that, the best parameter factor level combination is chosen.
7) The confirmation experiment is then carried out using the optimal parameter level combination.

The fundamental approach translates the objective parameter to the S/N ratio, which is used as the quality attributes assessment index in the Taguchi method parameter design. The S/N ratio is used to find the design with the least variance and the best performance. The final stage is to carry out the experiment to determine whether or not it was successful. Increase the factor weighting impact, decrease mutual action, process the average and variance concurrently, and improve engineering quality are all advantages of the S/N ratio. The higher the S/N ratio, the better the quality that may be achieved.

The responses are chosen so that they give an idea of how effective the etching process is, as well as the factors and levels that play a role in it. The workpiece's surface roughness and metal removal rate (MRR) can be used to figure out how well the etching process worked. Surface roughness and the rate at which metal is removed from the work piece are used to see how well the etching process works.

$$MRR = \frac{Initial\ weight\ of\ workpiece\ -\ Final\ weight\ of\ workpiece}{Machining\ time\ \mathrm{X}\ Density\ of\ 304\ stainless\ steel}$$

The goal of a quality improvement effort can be said to be trying to get the signal to noise (S/N) ratio for the product as high as possible. All of the responses that were used in this study should have bigger values for Surface roughness and Metal removal rate (MRR) after the etching process. So, to figure out the S/N ratio, the equation was used, and it's shown here:

$$\eta_{larger\ the\ better} = -10\log_{10}\left(\frac{1}{n}\sum_{i=1}^{n}\frac{1}{y_i^2}\right)$$

S. No. Control parameters	Level		
	1	2	3
Composition $X \mid Y$ (vol. %)	40 | 30	30 | 40	35 | 35
Temperature (˚C)	25	50	100
Soaking time (t)	1	3	5

Table 2: Experimental layout using the L_9 orthogonal array.

The etching solution is made up of X volume percent hydrochloric acid, Y volume percent phosphoric acid, and 30 volume percent distilled water.

The system's degree of freedom is computed and found to be 8. The L9 orthogonal array is a common orthogonal array that can support three levels and three factors. Taguchi's Quality Engineering Handbook provided the orthogonal array [8]. Tables 3. Shown the normal L9 Orthogonal array used in this study as well as the array with parameter level values.

Experiment No.	Compositions X/Y (Vol. %)	Temperature (˚C)	Soaking Time (minute)
1.	40/30	50	60
2.	40/30	75	90
3.	40/30	100	120
4.	30/40	50	90
5.	30/40	75	120
6.	30/40	100	60
7.	35/35	50	120
8.	35/35	75	60
9.	35/35	100	90

Table 3: L_9 Orthogonal array with parameters value.

The orthogonal arrays L_9 are used in this research, with the parameters and levels listed in Tables 2 and 3, respectively.

III. ANALYSIS OF DATA, RESULTS AND DISCUSSION

The experiments have been developed using Taguchi approach and are done and executed. The observations have been measured and the answers are computed as stated. The fluctuation of each answer with regard to each parameter that has been noticed and made an attempt to suggest causes for the variances. The output responses evaluated in this study are:

A. Evaluation of recast layer at microscopic level

During EDM, there will be a hard and brittle layer if the dielectric fluid did not flush away all of the molten metal that came from the workpiece during the process. They formed a thin layer on the periphery, that generated thin layer is known as a recast layer. If a layer is put on top of something, it can be anywhere from 2.5 to 50 microns thick. Figure 10 displays the photographs of the recast layer that may be acquired with the use of a vision measuring machine. This machine enables us to assess the surface qualities and their properties.

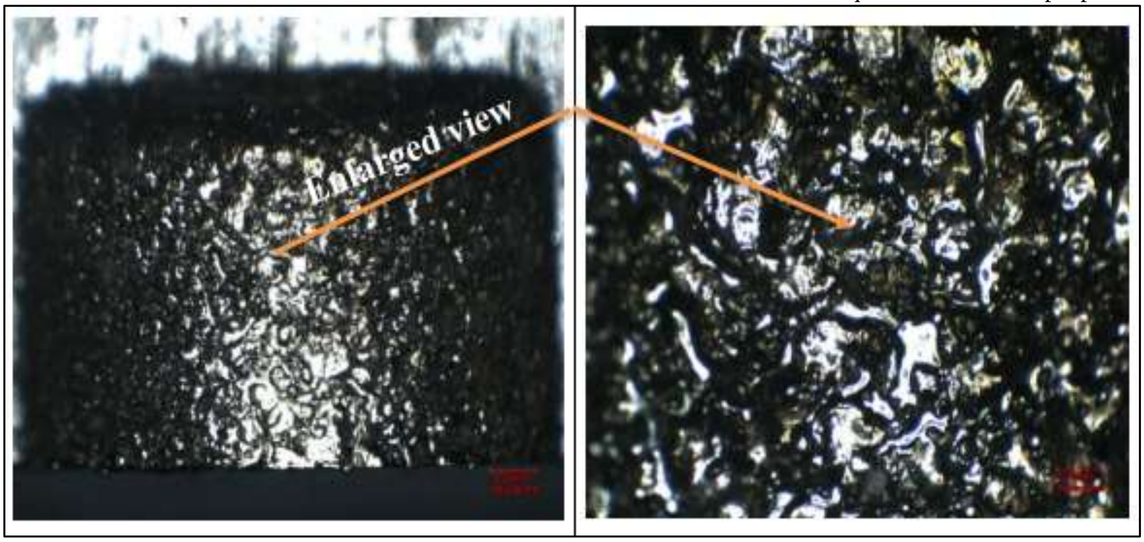

Fig. 10: Recast layer on the workpiece before etching

The recast layers so formed is extremely hard and brittle, and the surface is porous and may contain micro cracks which is not a good characteristic of a machined surface. Such surface should be removed before using these products. Figure 11 depicts images of the recast layer following the etching process, demonstrating how well the surface texture and properties will change.

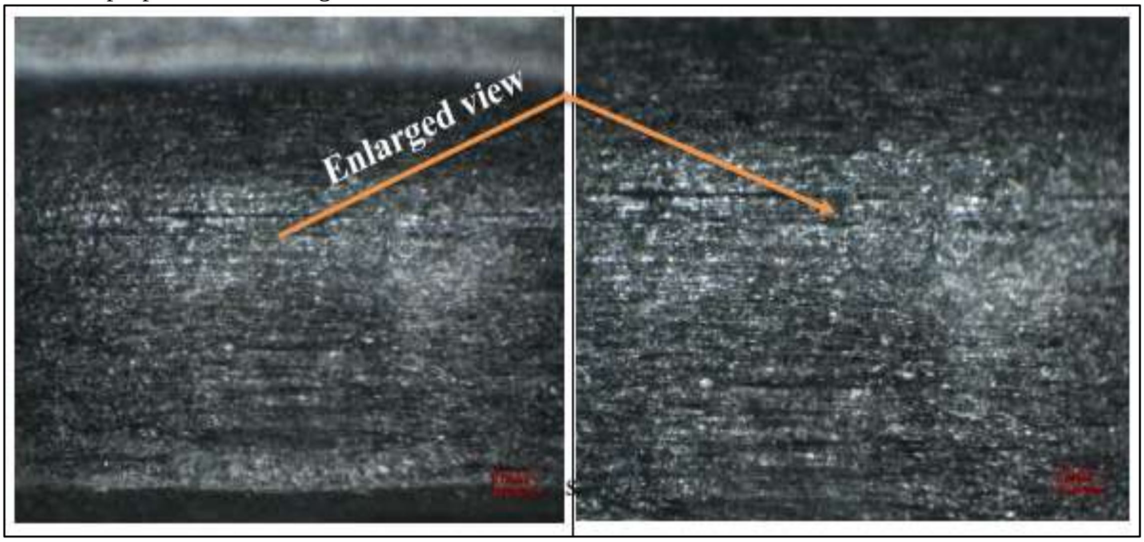

Fig. 11: Recast layer on the workpiece after etching

B. Analysis of etching and grinding process on recast layer cast layer

1) Analysis of metal removal rate (MRR)

Material removal rate (MRR) is the amount of material removed per time unit, directly aiming at the process productivity. In roughing operations and the production of large batches, this needs to be maximized. Weight loss occurs in both stages during the experiment. As a result, MRR will be computed separately for both circumstances, and the total MRR value will be the sum of both MRR values. Figure 12. Depicts the current state of the workpiece that may be employed in the experiments, as well as the etching process' influence on the workpiece.

Fig. 12: Comparison of workpiece before and after the etching process

To measure the value of MRR, weight of all the samples must be gathered after the etching and grinding operation. So, that the value of MRR may be computed with the aid of previously supplied formulae and MRR is expressed in mm3/min.

It is possible to compute the MRR value for both the processes separately and summation of both the MRR value (i.e. MRR value of etching and grinding process) can be used to calculate overall MRR value. Table 4. Shown the value of overall MRR.

Exp. No.	C	T	t	MRR value A E	MRR value A G	Overall MRR value
1	C1	50	60	0.8187	2.25	3.0688
2	C1	75	90	2.4333	4.5	6.9333
3	C1	100	120	2.7010	8.25	10.9510
4	C2	50	90	0.1528	3.75	3.9028
5	C2	75	120	0.2312	6.25	6.4813
6	C2	100	60	1.1667	6.75	7.9167
7	C3	50	120	0.0239	3.25	3.2740
8	C3	75	60	0.5208	6	6.5208
9	C3	100	90	1.5069	7.25	8.7569

Table 4: Overall MRR Value

Where, C = Acids Composition (X/Y/Z) vol %.
X = volume % of HCL, Y = volume % of H_3PO_4 and Z = volume % of distilled H_20 (in ml).
C1 = 40/30/30, C2 = 30/40/30 and C3 = 35/35/30
T = Temperature (^{0}C) and t = Soaking time (min).

Table 5. explains about the response table while calculating from the taguchi method. From this table we have to analyze which parameter is more effective for the particular process After applying taguchi analysis we get the value of S/N ratios which tells about the more effective parameters. So, from this table it can be concluded that temperature is more effective as compared to other parameters followed by soaking time and acid composition.

Levels	Composition	Temperature	Soaking time
1	15.34	10.62	14.67
2	15.14	16.45	15.83
3	15.78	19.20	15.77
Delta	0.64	8.58	1.17
Rank	3	1	2

Table 5: Overall MRR Response Table for Signal to Noise Ratios

Figure 13. depicts, S/N ratio value as "larger is better" condition from the taguchi analysis. In this graph, acid composition firstly is going to decrease and then increases as increases the HCl percentage. When reached 40% of hydrochloric acid composition along with 30% of phosphoric acid and 30% of distilled water, by which get the maximum S/N ratio value. From this we can conclude that 40% HCl by volume is more optimum for the etching process. From the same figure 12, for the temperature S/N value is maximum at 100 °C. The S/N ratio will increase if the temperature is increased. So, for this process 100 °C is more effective. Soaking time firstly slightly increases then decreases as we increase the soaking time. Soaking time is suitable for 90 minutes where, the maximum S/N value is achieved.

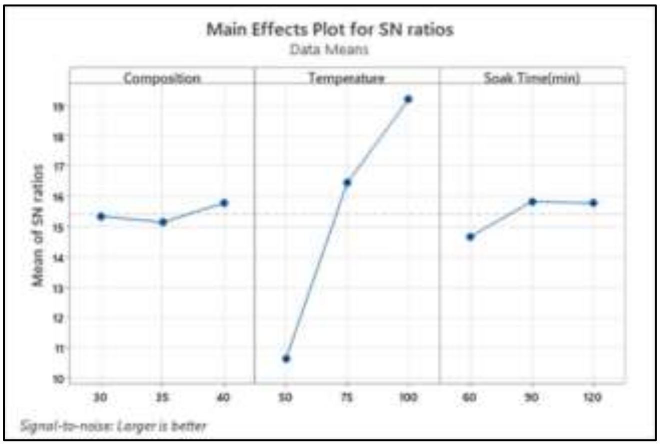

Fig. 13: S/N ratios main effects plot for MRR

Table 6. Represent the analysis of variance for MRR, through this analysis get the idea about the process or parameters which is more significant with respect to the others parameters. In this table, clearly observed that the contribution of temperature is more followed by soaking time and acid composition. There is a slight increment in soaking time as compared to the acidcomposition parameter. During the complete process, the contribution of temperature is 90.33%, soaking time is 3.14% and acid composition is 2.55%.

Source	DF	Sum of Squares	Mean Square	F-Value	P-Value	Contribution
Composition	2	1.429	0.7147	0.64	0.609	2.55%
Temp.	2	50.562	25.2808	22.74	0.042	90.33%
Soak Time	2	1.759	0.8797	0.79	0.558	3.14%
Error	2	2.223	1.1117			3.97%
Total	8					100.00%

Table 6: ANOVA and F test of RCL for MRR

2) Analysis of surface roughness (Ra)

The value of surface roughness before the etching process is larger as compared to the values after the etching process with all the respective experiments, from this conclude that after the etching process surface roughness value decreases. During the grinding process surface roughness value increases for some experiments and decreases for others.

Exp. No.	Composition	Temperature	Soaking time	Final Ra
1.	40	50	60	8.608
2.	40	75	90	8.429
3.	40	100	120	5.220
4.	30	50	90	5.065
5.	30	75	120	3.080
6.	30	100	60	3.054
7.	35	50	120	2.616
8.	35	75	60	2.477
9.	35	100	90	4.350

Table 7. Final Ra value after etching and grinding process

Table 7. Shows the value of surface roughness collected after the complete process for all the respectively experiment along with that Table 9. Shows the surface roughness value and their variation before and after the etching and grinding process respectively.

In Table 8, with the help of taguchi analysis when the Ra response table for S/N ratio is drawn the acid composition gets the highest priority followed by soaking time and temperature. It means that acid composition is more significant among all the parameters for the surface roughness value.

Levels	Composition	Temperature	Soaking time
1	11.187	13.714	12.091
2	9.667	12.055	15.126
3	17.189	12.274	10.826
Delta	7.522	1.659	4.300
Rank	1	3	2

Table 8. Ra Response Table for Signal to Noise Ratios

In figure 14, S/N ratio main effect plot for Ra is calculated using taguchi analysis, in which the "larger is better" for S/N ratio is chosen according to the desirable results. In this figure S/N ratio value for Ra value is firstly higher, lower in the middle and finally reaches to maximum value by the end as the acid composition increases.

In the same figure S/N ratio value for Ra is firstly higher than it decreases in the middle and it slightly increases with the increment in the temperature. In the same figure the S/N ratio value for Ra is maximum at 90 minutes, intermediate at 60 minutes and lowest at 120 minutes.

From all these statements above, it can be concluded that optimum S/N ratio value for Ra is achieved at 40 % of HCL, temperature is 50 ºC and 90 min. soaking time.

Exp. No.	Ra Graph Before Etching	Ra (µm)	Ra Graph After Grinding	Ra (µm)
1	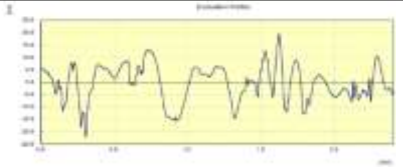	5.898	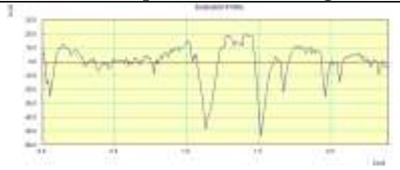	8.608
2	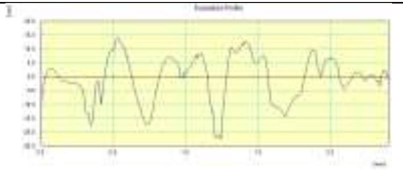	6.407	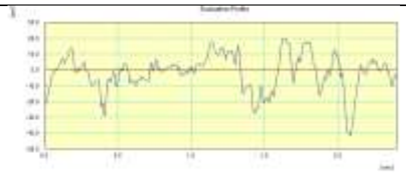	8.429
3	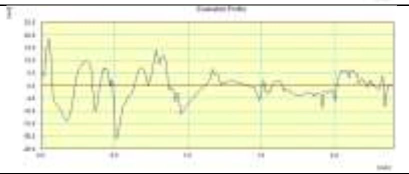	5.565	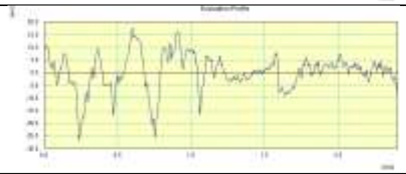	5.220
4	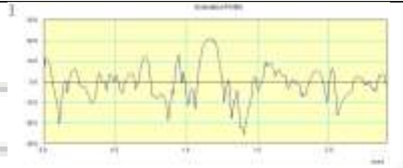	6.197	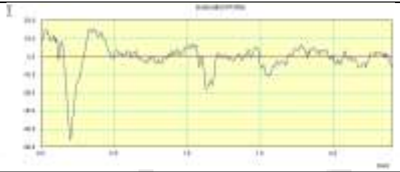	5.065
5	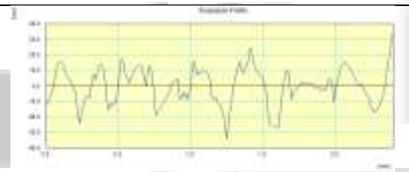	9.144	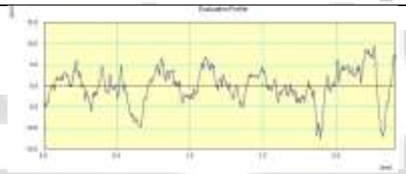	3.080
6	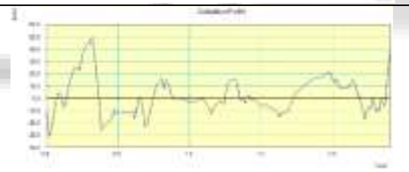	10.940	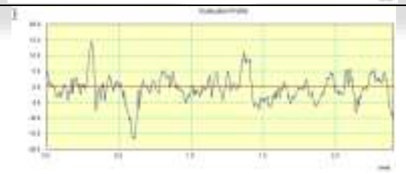	3.054
7	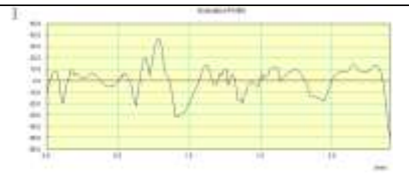	9.655	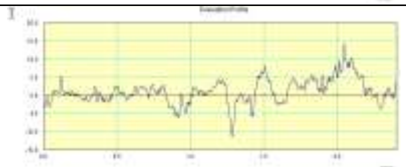	2.616
8	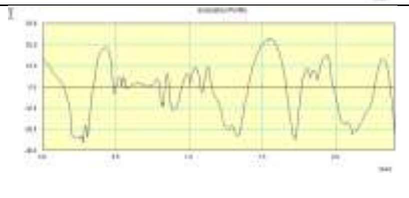	10.249	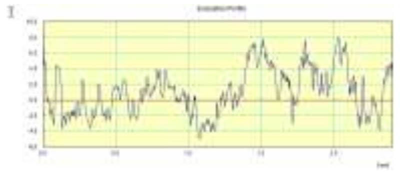	2.477
9	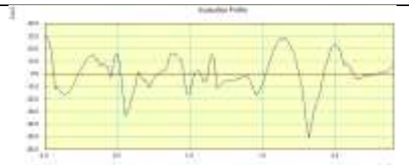	10.659	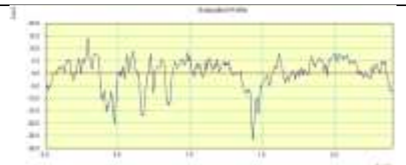	4.350

Table 9: Ra value and their variations for the experiment

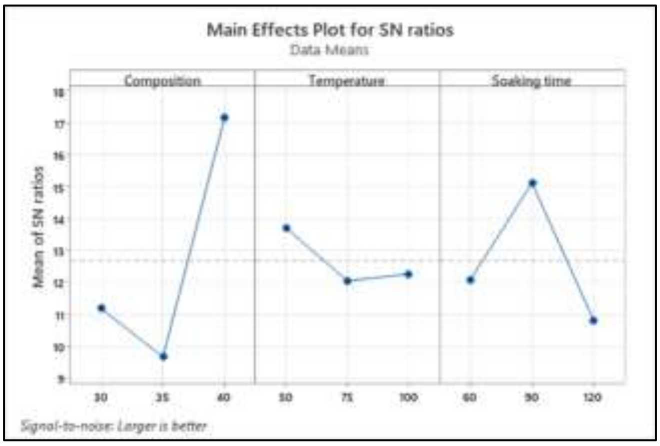

Fig. 14: S/N ratios main effects plot for Ra

Table 10. Represent the analysis of variance for Ra, through this analysis get the idea about the process or parameters which is more significant with respect to the others parameters for surface roughness value.

In this table, clearly observed that the contribution of acid composition is more followed by soaking time and temperature. There is a huge difference in contribution between the composition and temperature. During the complete removal process, the contribution of acid composition is 72.65 %, soaking time is 18.09 % and temperature is 5.17%.

Source	DF	Sum of Squares	Mean Square	F-Value	Contribution
Composition	2	32.173	16.0867	17.79	72.65%
Temp.	2	2.288	1.1439	1.26	5.17%
Soaking Time	2	8.012	4.0062	4.43	18.09%
Error	2	1.809	0.9044		4.08%
Total	8				100.00%

Table 10: ANOVA and F test of RCL for Ra

IV. CONCLUSION

This study employed the Taguchi experimental design to look at the feasibility of an EDM recast layer removal technique and the following research findings were reached.

1) The experiment was conducted using L9 orthogonal arrays and the results proved that metal removal rate is highly affected with temperature parameter followed by soaking time and acid compositions.
2) L9 orthogonal arrays were also used in the experiments and the results proved that the value of metal removal rate enhanced, under the proper temperature, soaking time and acid composition for 304 stainless steel and their alloys.
3) ANOVA analysis can be performed for the MRR value which gives the result that the contribution of temperature is more as compared to the other parameters for the removal of the recast layer.
4) Temperature is the most significant parameter from the response table of signal to noise ratio for the value of metal removal rate.
5) In the experiment, after performing the etching process the value of surface roughness increases but after the grinding process the value of surface roughness may increase or decrease
6) Analysis of variance can be performed for the Ra value which gives the result that the contribution of acid composition is very high among all the other parameters for the removal of the recast layer.
7) According to Taguchi analysis, Response table of signal to noise ratio explains that acid composition has more impact on the value of surface roughness as followed by soaking time and temperature.

V. REFERENCES

[1] Yildiz, Y. (2016). Prediction of white layer thickness and material removal rate in electrical discharge machining by thermal analyses. Journal of Manufacturing Processes, 23, 47–53. https://doi.org/10.1016/j.jmapro.2016.05.018.
[2] Yildiz, Y., Sundaram, M. M., Rajurkar, K. P., & Altintas, A. (2017). Correlation of surface roughness and recast layer thickness in electrical discharge machining. Proceedings of the Institution of Mechanical Engineers, Part E: Journal of Process Mechanical Engineering, 231(3), 414–424. https://doi.org/10.1177/0954408915600949.
[3] Gostimirovic, M., Kovac, P., Sekulic, M., & Skoric, B. (2012). Influence of discharge energy on machining characteristics in EDM. Journal of Mechanical Science and Technology, 26(1), 173–179. https://doi.org/10.1007/s12206-011-0922-x.
[4] Zhang, Y., Liu, Y., Ji, R., & Cai, B. (2011). Study of the recast layer of a surface machined by sinking electrical discharge machining using water-in-oil emulsion as dielectric. Applied Surface Science, 257(14), 5989–5997. https://doi.org/10.1016/j.apsusc.2011.01.083.
[5] Rao, G. K. M., Satyanarayana, S., & Praveen, M. (2008). Influence of machining parameters on electric discharge machining of maraging steels-An experimental investigation. Proceedings of the World Congress on Engineering, 2, 2–4.
[6] Rao, R. V. (2011). Advanced Modelling and Optimization of Manufacturing Processes”. In Springer Series in Advanced Manufacturing. Springer Verlag London Limited.
[7] Wang, C.-C., Chow, H.-M., Yang, L.-D., & Lu, C.-T. (2009). Recast layer removal after electrical discharge machining via Taguchi analysis: A feasibility study. Journal of Materials Processing Technology, 209(8),

4134–4140. https://doi.org/10.1016/j.jmatprotec.2008.10.012.

[8] Taguchi, G., Chowdhary, S., & Wu, Y. (2005). Taguchi's Quality Engineering handbook". John Wiley & Sons, Inc.

[9] Abbas, N. M., Solomon, D. G., & Bahari, M. F. (2007). A review on current research trends in electrical discharge machining (EDM). International Journal of Machine Tools and Manufacture, 47(7–8), 1214–1228.

[10] Abdulkareem, S., Khan, A. A., & Konneh, M. (2011). Influence of electrode cooling on recast layers and micro crack in EDM of titanium. Advanced Materials Research, 264–265, 1180–1186. https://doi.org/10.4028/www.scientific.net/amr.264-265.1180.

[11] Apte, P. R. (2011). Introduction to Taguchi methods", TRIZ workshop, Indian Institute of Technology. Chu, X., Zhuang, W., Xue, W., Quan, X., Zhou, W., & Fu, T. (2020).

[12] Electrolytic removal of recast layers on micro-EDM microstructure surfaces. The International Journal of Advanced Manufacturing Technology, 108(3), 867–879. https://doi.org/10.1007/s00170-020-05410-x.

[13] Gil, R., Sánchez, J. A., Plaza, S., Ortega, N., Izquierdo, B., & Pombo, I. (2014). Modeling recast layer and surface finish in the manufacturing of high–aspect ratio micro-tools using the inverse slab electrical discharge milling process. Proceedings of the Institution of Mechanical Engineers, Part B: Journal of Engineering Manufacture, 228(4), 553–562. https://doi.org/10.1177/0954405413502024.

[14] Guu, Y. H., Chou, C. Y., & Chiou, S.-T. (2005). Study of the effect of machining parameters on the machining characteristics in electrical discharge machining of Fe-Mn-Al alloy. Materials and Manufacturing Processes, 20(6), 905–916. https://doi.org/10.1081/amp-200060412.

[15] Guu, Y. H., Tsai, K.-L., & Chen, L.-K. (2007). An experimental study on electrical discharge machining of manganese–zinc ferrite magnetic material. Materials and Manufacturing Processes, 22(1), 66–70. https://doi.org/10.1080/10426910601015949.

[16] Holmberg, J., Wretland, A., & Berglund, J. (2016). Grit blasting for removal of recast layer from EDM process on inconel 718 shaft: An evaluation of surface integrity. Journal of Materials Engineering and Performance, 25(12), 5540–5550. https://doi.org/10.1007/s11665-016-2406-8.

[17] Kao, J. Y., Tsao, C. C., Wang, S. S., & Hsu, C. Y. (2010). Optimization of the EDM parameters on machining Ti–6Al–4V with multiple quality characteristics. The International Journal of Advanced Manufacturing Technology, 47(1–4), 395–402. https://doi.org/10.1007/s00170-009-2208-3.

[18] Katz, Z., & Tibbles, C. J. (2005). Analysis of micro-scale EDM process". International Journal of Advanced Manufacturing Technology, 25, 923–928.

[19] Kibria, G., Sarkar, B. R., Pradhan, B. B., & Bhattacharyya, B. (2010). Comparative study of different dielectrics for micro-EDM performance during microhole machining of Ti-6Al-4V alloy. The International Journal of Advanced Manufacturing Technology, 48(5–8), 557–570. https://doi.org/10.1007/s00170-009-2298-y.

[20] Kumar, A., Kumar, V., & Kumar, J. (2016). Surface crack density and recast layer thickness analysis in WEDM process through response surface methodology. Machining Science and Technology, 20(2), 201–230. https://doi.org/10.1080/10910344.2016.1165835.

[21] Lim, H. S., Wong, Y. S., Rahman, M., & Lee, M. K. E. (2003). A Study on the machining of high aspect ratio micro-structures using Micro-EDM". Journal of Materials Processing Technology, 140, 318–325.

[22] Liu, H. S., Yan, B. H., Huang, F. Y., & Qiu, K. H. (2005). A study on the characterization of high nickel alloy micro-holes using micro EDM and their applications". Journal of Materials Processing Technology, 169, 418–426.

[23] Montgomery, D. C. (2001). Design and Analysis of Experiments". John Wiley & Sons, Inc.

[24] Newton, T. R. (2008). Investigation of the effect of process parameters on the formation of recast layer in wire-EDM of Inconel 718 (Doctoral dissertation).

[25] Newton, Thomas R., Melkote, S. N., Watkins, T. R., Trejo, R. M., & Reister, L. (2009).

[26] Investigation of the effect of process parameters on the formation and characteristics of recast layer in wire-EDM of Inconel 718. Materials Science & Engineering. A, Structural Materials: Properties, Microstructure and Processing, 513–514, 208–215. https://doi.org/10.1016/j.msea.2009.01.061.

[27] Pandey, A., & Singh, S. (2010). Current research trends in variants of Electrical Discharge Machining: A review. International Journal of Engineering Science and Technology, 2(6), 2172–2191.

[28] Patel, * Pandey, K. M., & Rao, P. M. (2009). Determination of an optimum parametric combination using a surface roughness prediction model for EDM of Al2O3/SiCw/TiC ceramic composite. Materials and Manufacturing Processes, 24(6), 675–682.

[29] Phadke, M. S. (1999). Quality Engineering using Robust Design". Prentice Hall Inc.

[30] Pradhan, B. B., Masanta, M., Sarkar, B. R., & Bhattacharyya, B. (2009a). Investigation of electro discharge micro-machining of titanium super alloy". International Journal of Advanced Manufacturing Technology, 41, 1094–1106.

[31] Pramanik, A., Basak, A. K., Prakash, C., Shankar, S., Sharma, S., & Narendranath, S. (2021). Recast layer formation during wire electrical discharge machining of titanium (ti-Al6-V4) alloy. Journal of Materials Engineering and Performance, 30(12), 8926–8935. https://doi.org/10.1007/s11665-021-06116-1.

[32] Rajurkar, K. P., Levy, G., Malshe, A., Sundaram, M. M., Mcgeough, J., Hu, X., Resnick, R., & Desilva, A. (2006). Micro and Nano Machining by Electro-Physical and Chemical Processes". Annals Of The CIRP, 55(2), 643–666.

[33] Ross, P. J. (1996). Taguchi techniques for quality engineering". McGraw-Hill Companies Inc.

[34] Singh, S., & Pandey, A. (2013). Some studies into electrical discharge machining of Nimonic75 super alloy

using rotary copper disk electrode. Journal of Materials Engineering and Performance, 22(5), 1290–1303. https://doi.org/10.1007/s11665-012-0412-z.

[35] Tai, T., & Lu, S. (2009). Improving the fatigue life of electro-discharge-machined SDK11 tool steel via the suppression of surface cracks. International Journal of Fatigue, 31(3), 433– 438. https://doi.org/10.1016/j.ijfatigue.2008.07.013.

[36] Vignesh, S., Mohan, B., Muthuramalingam, T., & Karthikeyan, S. (2015). Evaluation of recast layer thickness of electrical discharge machined AISI 202 stainless steel with various pulse generators. Applied Mechanics and Materials, 766–767, 518–522. https://doi.org/10.4028/www.scientific.net/amm.766-767.518.

[37] Xu, B., Chen, S.-G., Liang, X., Lei, J.-G., Shi, H.-Y., Fu, L.-Y., Yang, J., Peng, T.-J., Zhao,

[38] H., & Zhu, L.-K. (2020). Recast layer removal of 304 stainless steel by combining micro- EDM with negative polarity micro-EDM. The International Journal of Advanced Manufacturing Technology, 107(11–12), 4713–4723 https://doi.org/10.1007/s00170-020- 05312-y.

[39] Yan, B. H., Wang, C. C., Chow, H. M., & Lin, Y. C. (2000). Feasibility study of rotary electrical discharge machining with ball burnishing for Al2O3/6061Al composite. International Journal of Machine Tools & Manufacture, 40(10), 1403–1421. https://doi.org/10.1016/s0890-6955(00)00005-5.

[40] Yu, Z., Rajurkar, K. P., & Narasimhan, J. (2003). Effect of machining parameters on machining performance of micro EDM and surface integrity". In Proceedings of Annual ASPE Meeting.